


 Cite this: *Chem. Commun.*, 2025, 61, 8596

 Received 22nd January 2025,  
 Accepted 10th March 2025

DOI: 10.1039/d5cc00425j

rsc.li/chemcomm

# Reductive alkylation of azoarenes to *N*-alkylated hydrazines enabled by hexafluoroisopropanol†

 Siddhartha Kumar Senapati and Animesh Das \*

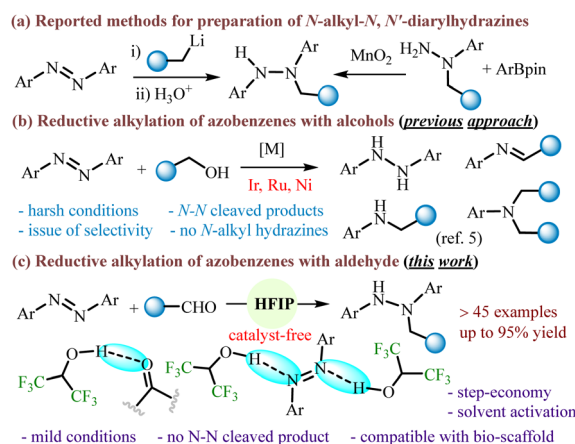
**A one-pot tandem approach to *N*-alkyl-*N,N'*-diarylhydrazines was developed using a sequence of reduction of azoarene to hydrazone followed by reductive alkylation by an aldehyde. The mild reaction conditions suppress *N–N* cleaved products and selectively provide trisubstituted hydrazine derivatives. The mechanistic study demonstrates that the iminium formation step is likely to be the rate-limiting step.**

Hydrazine derivatives are an important class of compounds that are widely utilized in the pharmaceutical, agrochemical, polymer and dye industries.<sup>1</sup> They also have useful synthetic applications in the synthesis of nitrogen-containing compounds and coupling reactions.<sup>2</sup> Nevertheless, the synthesis of target-based *N*-alkyl-*N,N'*-diarylhydrazines is difficult, which seriously restricts their bioactivity and application research. The reported methods are the addition of alkyllithium to the N=N bond of an azobenzene under cryogenic conditions or the oxidative coupling of *N*-alkyl-*N*-arylhydrazines with aryl borates (Scheme 1a).<sup>3</sup> Therefore, it is deemed desirable to develop a mild and efficient method for the construction of *N*-alkyl-*N,N'*-diarylhydrazines without the use of reactive organolithium reagents, expensive borates, and external oxidants.

Direct N=N functionalization of azobenzenes is one of the promising synthetic approaches to synthesize *N,N'*-diaryl hydrazine derivatives and various *N*-heterocycles. However, unlike highly reactive alkyl azodicarboxylates with a strongly electrophilic N=N double bond, azobenzenes typically exist in a stable and nonpolar *trans* form, showing low N=N bond reactivity.<sup>4</sup> In a recent study, transition-metal catalyzed reductive alkylation of azobenzenes with alcohols is attempted for the construction of *N*-alkyl-*N,N'*-diarylhydrazines (Scheme 1b).<sup>5</sup> However, the process failed to obtain the desired hydrazine and

led to the formation of *N–N* cleaved products. The over-reduction of azoarenes to amine derivatives renders the process less efficient for the synthesis of *N*-alkylated hydrazine. Besides, the methods require the use of transition metal catalysts, harsh conditions, and lack of tolerance with hydrogenation-sensitive functional groups. Therefore, we were interested to develop a mild and efficient method for the construction of substituted hydrazine derivatives under catalyst-free conditions with a wide range of substrate scopes.

The use of 1,1,1,3,3,3-hexafluoroisopropanol (HFIP) has recently gained attention because of their unique physical and chemical properties (such as low nucleophilicity, high ionizing power, strong hydrogen-bond donor ability and cation stabilization).<sup>6</sup> This is believed to be considered as an ideal reaction medium in promoting various reactions under mild conditions including unsaturated carbon-carbon bond functionalization,<sup>6f</sup> C–H functionalization,<sup>6d,e</sup> hydroarylation,<sup>7</sup> *N*-alkylation,<sup>8</sup> *C*-alkylation reaction<sup>9</sup> and aza-Piancatelli cyclization.<sup>10</sup> Nevertheless, the use of HFIP only as an activator has received limited attention in reduction chemistry.



**Scheme 1** Alkylation of azoarenes and synthesis of *N*-alkyl-*N,N'*-diarylhydrazines.

Department of Chemistry, Indian Institute of Technology Guwahati, Guwahati-781039, Assam, India. E-mail: adas@iitg.ac.in

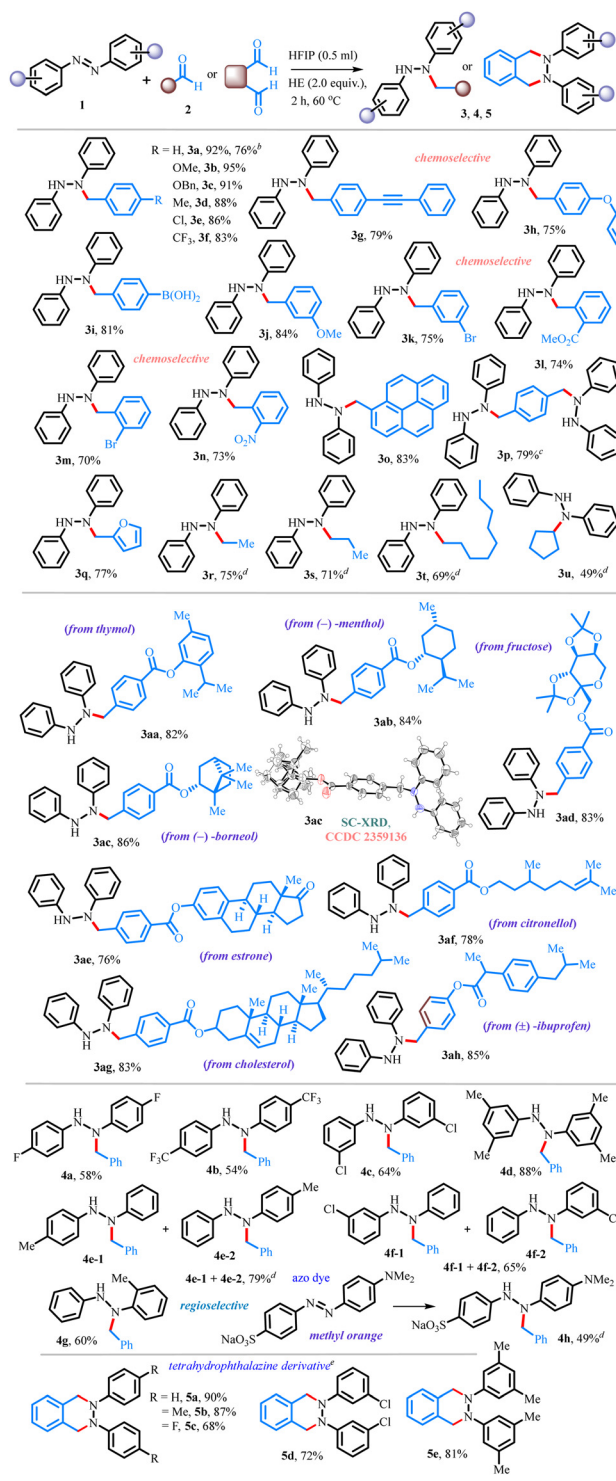
 † Electronic supplementary information (ESI) available. CCDC 2359136. For ESI and crystallographic data in CIF or other electronic format see DOI: <https://doi.org/10.1039/d5cc00425j>


Herein, we envisaged that the strong H-bond donor properties of HFIP can not only aid in the hydrogenation of azoarenes to hydrazoarenes but also in the reductive *N*-alkylation of the resulting compounds (Scheme 1c). Our investigation initiated with the reaction of azobenzene (**1a**, 0.5 mmol), benzaldehyde (**2a**, 0.5 mmol), and Hantzsch ester (HE) (1 mmol) in HFIP (0.1 mL) at 60 °C. After 2 h, *N*-alkylated hydrazine **3a** was obtained in 22% yield, along with 32% intermediate hydrogenated product hydrazobenzene (**1a'**, Table 1, entry 1). To improve the yield of desired product **3a**, the equivalency of HFIP was gradually increased (entry 2). When HFIP was used in 0.5 mL, product **3a** was obtained in 92% yield (entry 3). A decrease in the yield of **3a** has been observed when the reaction was examined with a mixture of solvents (entries 4–6). The yield of **3a** was also decreased by reducing the reaction time (entry 7) or by reducing the reaction temperature (entry 8). Then, the reaction was examined with  $-\text{CF}_3$  functionalized thiourea as a hydrogen-bond donor catalyst in DCE, providing the product **3a** in 60% yield, indicating that the hydrogen-bonding donor property is important in this transformation (entry 9). We have examined the reaction by replacing HFIP with a relatively weak hydrogen bond donor solvent, isopropanol, which failed to provide any desired product (entry 10). This reiterates the significance of the role of HFIP in the current transformation as a strong H-bond donor solvent. We next intended to explore the scope of the *N*-alkylation reaction with a variety of aldehydes **2a–t**, **2aa–ah** using **1a** as the standard substrate (Table 2). The substrates having both electron-donating (e.g.,  $-\text{Me}$ ,  $-\text{OMe}$ ,  $-\text{OBn}$ ) and electron-withdrawing groups (e.g.,  $-\text{Cl}$ ,  $-\text{CF}_3$ ) at the *para*-position in the aryl moiety were efficiently reacted to obtain the desired products **3a–3f** in 83–92% yields. Slightly higher yields were realized for electron-donating groups. With boronic acid containing aldehyde, the desired product **3i** was formed with 81% yield. Since, the present reaction conditions tolerate the  $-\text{B}(\text{OH})_2$  group functional groups, it can be useful for further functionalization in

Table 1 Optimization studies<sup>ab</sup>

Entry	Deviation from standard conditions	Yield (%)
1	HFIP (0.1 mL)	22%, (32% of <b>1a'</b> )
2	HFIP (0.2 mL, 0.3 mL, 0.4 mL)	41%, 65%, 81%
3	None	92%
4	HFIP : DCE (1 : 3, 0.5 mL)	25%
5	HFIP : CH <sub>3</sub> OH (1 : 3, 0.5 mL)	21%
6	HFIP : toluene (1 : 3, 0.5 mL)	18%
7	With 0.5 h, 1 h, 1.5 h	26%, 48%, 74%
8	At 25 °C, at 45 °C	0%, 14%
9 <sup>b</sup>	With HBD catalyst	60%
10	With isopropanol (0.5 mL)	0%

<sup>a</sup> Reaction conditions: **1a** (0.5 mmol), **2a** (0.5 mmol), HE (1 mmol) in HFIP (0.5 mL) at 60 °C for 2 h under Ar, isolated yields. <sup>b</sup> With HBD catalyst 1,3-bis(3,5-bis(trifluoromethyl)phenyl)thiourea (15 mol%) in DCE (0.5 mL).

Table 2 Substrate scope<sup>ab</sup>

<sup>a</sup> Reaction conditions: **1** (0.5 mmol), aldehyde or ketone (0.5 mmol), HE (1 mmol), HFIP (0.5 mL), at 60 °C for 2 h, isolated yields. <sup>b</sup> 2 mmol scale. <sup>c</sup> With 0.25 mmol of terephthalaldehyde, HE (4 equiv.). <sup>d</sup> 0.25 mmol scale. <sup>e</sup> With HE (3.2 equiv.).

Pd-catalyzed Suzuki–Miyaura cross-coupling reaction. Furthermore, *meta*- and *ortho*-substituent bearing aldehydes afforded the corresponding hydrazine products **3j–3k**, **3l–3n** in moderate to good

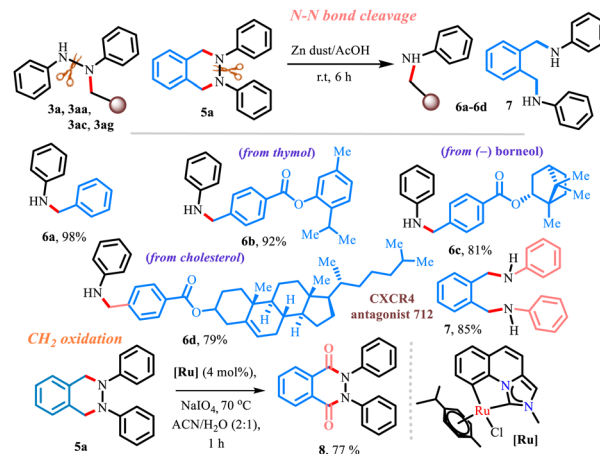


yields. Notably, the retention of reducible-functional groups (4-Cl, 4-OBn, 4-CF<sub>3</sub>, 4-C≡CPh, 4-O-allyl, 3-Br, 2-Br, 2-CO<sub>2</sub>Me, 2-NO<sub>2</sub>) in the final products showcases the excellent chemoselectivity of the present reductive protocol. Interestingly, 1-pyrene aldehyde also led to the products **3o** in 83% yields. When 1,4-benzenedialdehyde was used as an alkylating agent the poly *N*-alkylated hydrazine **3p** was readily obtained with notable selectivity. Besides aromatic aldehydes, the scope of the reaction was expanded to heteroaromatic aldehydes and a variety of aliphatic aldehydes and cyclic ketones, yielding **3q–3t** and **3u**. Considering the efficiency of the present protocol, the scope of the reaction was further expanded using highly functionalized substrates with complex molecular settings.

A range of biologically relevant motifs (BRM) were tested and were independently subjected to the optimized reaction conditions, affording the corresponding hydrazine derivatives containing thymol (**3aa**, 82%), (–)-menthol (**3ab**, 84%), (–)-borneol (**3ac**, 86%), fructose (**3ad**, 83%), estrone (**3ae**, 76%), citronellol (**3af**, 78%), cholesterol (**3ag**, 83%), and (±)-ibuprofen (**3ah**, 85%) moieties. The structure of the product **3ac** was further confirmed by single-crystal X-ray diffraction analyses. This suggests that there are no structural (chemical and stereochemical) changes of the complex architecture in the entity. To further demonstrate the generality and practicability of this reaction, a range of azobenzenes **1b–1g** were tested. Substituted symmetrical azobenzenes having *p*-F (**1b**), *p*-CF<sub>3</sub> (**1c**), *m*-Cl (**1d**) and *m,m'*-(CH<sub>3</sub>)<sub>2</sub> (**1e**) all efficiently provided the corresponding alkylated products **4a–4d** in 54–88% yields. On the other hand, unsymmetrical azobenzenes **1f** and **1g** provided an inseparable mixture of the alkylated products **4e** and **4f** in 81% and 65%, respectively, whereas *ortho*-substituted azobenzene **1h** afforded a single regioisomeric product **4g** in 60% yield. The methodology was further extended towards commercially used azo dyes such as methyl orange, obtaining *N*-alkylated product **4h** in 49% yield. It's worth mentioning that when the reaction was examined with phthalaldehyde under standard conditions, biologically relevant tetrahydrophthalazine derivatives **5a–5e** were obtained in 68–90% yields. Additionally, the reaction was shown to work effectively on a 2 mmol-scale (see ESI,† Scheme S8), and the method displays the convenient regeneration of the Hantzsch ester by re-reducing the aromatized by-product (see ESI,† Schemes S9 and S10).

Furthermore, the synthesized molecules can be easily transformed into useful molecules (Scheme 2). For example, *N–N* bond cleavage of various hydrazine derivatives **3a**, **3aa**, **3ac** and **3ag** proceeded smoothly using Zn in AcOH, delivering the secondary amines **6a–6d** in moderate to good yields. It is worth mentioning that the current reductive approach is applicable for the synthesis of secondary amines **6b–6d** with complex molecular settings. Compound **5a** can also be easily transformed into CXCR4 antagonist **712**<sup>11</sup> (**7**, 85% yield) *via* *N–N* bond cleavage. Furthermore, compound **5a** was converted to 2,3-diphenyl-2,3-dihydro phthalazine-1,4-dione **8** (77%) under oxidative conditions by a cyclometalated ruthenium catalyst and periodate.<sup>12</sup>

The mechanism of reaction was studied noting the hydrogen bond donor properties of HFIP (Fig. 1). Close investigation of



Scheme 2 Post synthetic modification and reductive *N–N* bond cleavages.

the nature of binding in solution shows that there is a weak hydrogen bond interaction between –OH of HFIP and the N-atom of the azobenzene moiety. It was confirmed by the <sup>1</sup>H NMR with a downfield shift (from  $\delta = 3.21$  to 3.61 ppm) of the signal of –OH protons in HFIP along with a weak upfield shift (from  $\delta = 4.39$  to 4.31 ppm) of the signal of the –CH proton in HFIP (Fig. S1, ESI†). The signals corresponding to *ortho*-aromatic protons in **1a** were slightly shifted in the upfield ( $\Delta\delta$  0.2 ppm).<sup>13</sup> Then, interaction of HFIP with the freshly distilled aldehyde and carbonyl group in HE was also confirmed by <sup>1</sup>H and <sup>13</sup>C NMR, and IR spectroscopic experiments (Fig. S2–S4, ESI†). Upon addition of aldehyde **2f**,<sup>14</sup> the hydroxyl peak of HFIP was shifted downfield by nearly 0.52 ppm in the <sup>1</sup>H NMR, and the carbonyl value moved downfield ( $\Delta\delta$  2.76 ppm) in the <sup>13</sup>C NMR. Furthermore, the carbonyl band shifted to a lower frequency (from 1708 to 1694 cm<sup>–1</sup>) in the IR spectrum. Experimental observation suggests that there is a weak hydrogen bonding interaction between HFIP and the aldehyde group.<sup>14</sup> Likewise, interaction of HFIP with the carbonyl group in HE was also validated by <sup>13</sup>C NMR with a downfield shift ( $\Delta\delta$  0.7 ppm) (Fig. S5 and S6, ESI†).

Next, a few control experiments were carried out to gain mechanistic insights into the synthesis of hydrazine derivatives (see ESI,† Section S8.4). The reaction of azobenzene **1a** in the absence of aldehyde under standard conditions afforded 1,2-diphenyl hydrazine **1a'** in 98% yield. For the subsequent step, the reaction was conducted with the formed **1a'**, and aldehyde **2a** under standard conditions and the desired product **3a** was obtained in 87% yield (Scheme S11, ESI†), from which it can be

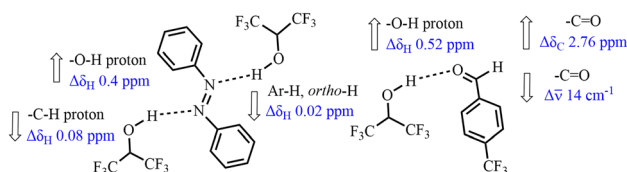
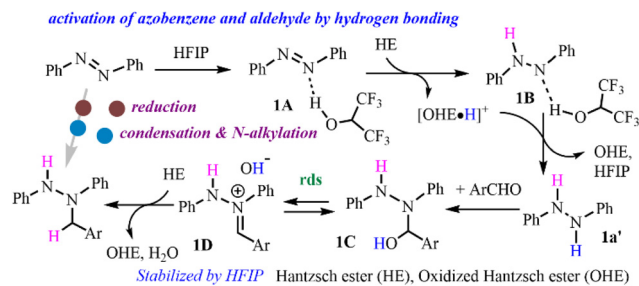


Fig. 1 Interaction of HFIP with **1a** and aldehyde **2f** by NMR and IR studies.





Scheme 3 Proposed pathway for the formation of *N*-alkylated hydrazine.

inferred that the reaction possibly occurs in two steps *i.e.*, reduction of azobenzene, followed by reductive *N*-alkylation of hydrazobenzene to *N*-alkylated hydrazine. Then, the electronic effect of the substrate on the rate of the reaction was examined (Scheme S12 and S13, ESI<sup>†</sup>). A competitive reaction suggested that the electron-donating group bearing a substituent (*-Me*) on the azobenzene enhanced the rate of the reaction with respect to an electron-withdrawing group (*p-F*). Likewise, an electron-donating group (*p-OMe*) on the benzaldehyde enhanced the rate of the reaction with respect to an electron-withdrawing group (*p-Cl*). In contrast, there is no considerable effect of electronics on the rate of the reaction in the azobenzene hydrogenation step (see ESI<sup>†</sup>, Section S12). Furthermore, we have investigated the kinetic Hammett correlation study using various *para*-substituted benzaldehydes under standard reaction conditions (see ESI<sup>†</sup>, Section S8.7). The reaction rates are in the order OMe > Me > H > Cl. The least-squares fit to the plot of  $[\log(k_X/k_H)]$  vs. Hammett  $\sigma^+$  constant gave a straight line with a  $\rho^+$  value of  $-1.3$ . A negative  $\rho^+$  value suggests that in the transition state, electrons are flowing away, which is stabilised by the electron-donating substituents. The effect of temperature on the rate of condensation reaction was examined by using Eyring analysis (see ESI<sup>†</sup>, Section S8.8). The activation parameters were found to be  $\Delta H^\ddagger = 29.2 \pm 1.6 \text{ kcal mol}^{-1}$  and  $\Delta S^\ddagger = +12.02 \pm 0.9 \text{ cal K}^{-1} \text{ mol}^{-1}$ . The positive entropy of activation suggests that the involvement of a dissociative process is the turnover-limiting step. Based on the thermodynamic activation parameters, kinetic Hammett studies, and competitive reaction on the substrate, one can postulate that the iminium formation step is likely to be the rate-limiting step.

On the basis of the above experimental findings, a proposed pathway for the formation of *N*-alkylated hydrazine has been demonstrated in Scheme 3. First, the azobenzene **1a** is activated by the hydroxyl group of HFIP *via* hydrogen bonding interaction, which is then reduced by Hantzsch ester to provide hydrazobenzene **1a'**. The *in situ* generated hydrazobenzene can react with aldehyde to form hemiaminal species **1c**, followed by condensation leading to the formation of iminium intermediate **1d**. Then, this was readily reduced by Hantzsch ester to provide the *N*-alkylated hydrazine **3a**.

In summary, catalyst-free HFIP-promoted one-pot tandem reduction of azoarene with subsequent reductive alkylation using aldehydes to form *N*-alkylated hydrazine derivatives has

been demonstrated. The protocol shows notable selectivity as the formation of *N-N* cleaved product amines and/or imines is completely suppressed. A wide range of functional group tolerance and structural features encountered in pharmaceuticals was demonstrated. This study demonstrates the general utility of HFIP in reduction chemistry.

A. D. gratefully acknowledges the SERB, DST (CRG/2022/01606) and SR/FST/CS-II/2017/23c) for the financial support.

## Data availability

The data supporting this article have been included as part of the ESI<sup>†</sup>.

## Conflicts of interest

There are no conflicts to declare.

## Notes and references

- (a) U. Ragnarsson, *Chem. Soc. Rev.*, 2001, **30**, 205–213; (b) N. Raziq, M. Saeed, M. S. Ali, M. Shahid, M. Lateef and S. Zafar, *Nat. Prod. Res.*, 2022, **36**, 961–966.
- (a) S. Balgotra, P. K. Verma, R. A. Vishwakarma and S. D. Sawant, *Catal. Rev.*, 2020, **62**, 406–479; (b) Y. Kong, K. Wei and G. Yan, *Org. Chem. Front.*, 2022, **9**, 6114–6128.
- (a) A. R. Katritzky, J. Wu and S. V. Verin, *Synthesis*, 1995, 651–653; (b) A. Yanagisawa, T. Sawae, S. Yamafuji, T. Heima and K. Yoshida, *Synlett*, 2015, 1073; (c) J. Wang, D. Wang and X. Tong, *Org. Biomol. Chem.*, 2021, **19**, 5762–5766.
- F. A. Jerca and V. V. Jerca, *Nat. Rev. Chem.*, 2022, **6**, 51–69.
- (a) S. Bansal, R. G. Gonnade and B. Punji, *Catal. Sci. Technol.*, 2023, **13**, 2705–2713; (b) I. Borthakur, M. Maji, A. Joshi and S. Kundu, *J. Org. Chem.*, 2022, **87**, 628–643; (c) D. Gong, D. Kong, N. Xu, Y. Hua, B. Liu and Z. Xu, *Org. Lett.*, 2022, **24**, 7339–7343.
- (a) H. F. Motiwala, A. M. Armaly, J. G. Cacioppo, T. C. Coombs, K. R. K. Koehn, V. M. Norwood IV and J. Aubé, *Chem. Rev.*, 2022, **122**, 12544–12747; (b) I. Colomer, A. E. R. Chamberlain, M. B. Haughey and T. J. Donohoe, *Nat. Rev. Chem.*, 2017, **1**, 0088; (c) X. D. An and J. Xiao, *Chem. Rec.*, 2020, **20**, 142–161; (d) S. K. Sinha, T. Bhattacharya and D. Maiti, *React. Chem. Eng.*, 2019, **4**, 244–253; (e) T. Bhattacharya, A. Ghosh and D. Maiti, *Chem. Sci.*, 2021, **12**, 3857–3870; (f) S. Ghosh, K. Patra and M. Baidya, *Eur. J. Org. Chem.*, 2024, e202301321.
- Selected examples: (a) C. Qi, V. Gandon and D. Leboeuf, *Angew. Chem., Int. Ed.*, 2018, **57**, 14245–14249; (b) L. Hu, Y. Liu, X. Fang, Y. Zheng, R. Z. Liao, M. Li and Y. Xie, *ACS Catal.*, 2022, **12**, 5857–5863.
- Selected examples: (a) Z. Zhang, X. Zhang, Y. Liu, X. Wang and X. Zhang, *J. Org. Chem.*, 2023, **88**, 14189–14192; (b) T. Lebleu, X. Ma, J. Maddaluno and J. Legros, *Chem. Commun.*, 2014, **50**, 1836–1838.
- (a) S. Wang, G. Force, R. Guillot, J. F. Carpentier, Y. Sarazin, C. Bour, V. Gandon and D. Leboeuf, *ACS Catal.*, 2020, **10**, 10794–10802; (b) H. Song, H. Zhou, Y. Shen, H. Wang, H. Song, X. Cai and C. Xu, *J. Org. Chem.*, 2022, **87**, 1086–1097.
- D. Leboeuf, L. Marin, B. Michelet, A. Perez-Luna, R. Guillot, E. Schulz and V. Gandon, *Chem. – Eur. J.*, 2016, **22**, 16165–16171.
- W. Q. Zhan, Z. X. Liang, A. Z. Zhu, S. Kurtkaya, H. Shim, J. P. Snyder and D. C. Liotta, *J. Med. Chem.*, 2007, **50**, 5655–5664.
- M. Konwar, T. Das and A. Das, *Org. Lett.*, 2024, **26**, 1184–1189.
- Yu. A. Mikheeva and Yu. A. Ershov, *Russ. J. Phys. Chem. A*, 2018, **92**, 1499–1507.
- (a) J. Gaster, S. Kozuch and D. Pappo, *Angew. Chem., Int. Ed.*, 2017, **56**, 5912–5915; (b) J. Khan, N. Taneja, N. Yadav and C. K. Hazra, *Chem. Commun.*, 2024, **60**, 11367–11370.

